Carbohydrate Polymers 87 (2012) 1913–1918

Contents lists available at SciVerse ScienceDirect

Carbohydrate Polymers

journal homepage: www.elsevier.com/locate/carbpol

Preparation, characterization and *in vitro* anti-metastasis activity of glucan derivatives

Ting Wang [1], Hongping Yin [1], Wenyi Wang, Min Wang *

Department of Microbiology and Biochemistry (Room 4407), School of Life Science and Technology, China Pharmaceutical University, 210009, Jiangsu, China

ARTICLE INFO

Article history:
Received 18 August 2011
Received in revised form
22 September 2011
Accepted 27 September 2011
Available online 5 October 2011

Keywords:
Glucan
Heparanase
Basic fibroblast growth factor

ABSTRACT

Four derivatives (PSC, PSC1, PMC and PMC1) with different substitution were prepared from β-(1→3)-D-glucan or carboxymethyl glucan using modified Wolfrom's method and characterized by homogeneity analysis, molecular weight analysis and elemental analysis. The structure of PSC was confirmed by FTIR and ^{13}C NMR. FTIR spectrum of PSC showed the characteristic absorptions of sulfate ester bonds at 807 cm^{-1} and 1210 cm^{-1}. ^{13}C NMR spectrum indicated the relatively high substitution degree at C-6 position. The heparanase inhibitory activities of four derivatives were predicted by docking to a homology model of heparanase. The result of the heparanase assay *in vitro* supported the computer prediction. Of these, PSC (8,000 Da, DS = 2.6) showed the high inhibitory activity. In further investigations, it was found that PSC remarkably inhibited the bFGF induced migration of HUVECs and MDA-MB-435. The result of the Western blotting revealed that PSC blocked basic fibroblast growth factor (bFGF) signal transduction pathway by decreasing the phosphorylation of ERK 1/2 and JNK.

1. Introduction

Tumor invasion and metastasis are complex processes which involve the critical steps of degrading basement membrane (BM) and extracellular matrix (ECM) (Yurchenco & Schittny, 1990). BM and ECM consist of collagen, fibronectin, laminin, vitronectin, heparin sulfate glycosaminoglycans (HSPGs), etc. HSPGs play an important role in regulating many physiological processes such as adhesion, migration, differentiation, and proliferation. HSPGs serve as structural barriers of the BM and ECM (Kjellen & Lindahl, 1991; Jackson, Busch, & Cardin, 1991). Heparin sulfate (HS) chains of HSPGs can also bind and sequester growth factors (i.e., bFGF and VEGF) (Vlodavsky, Miao, Medalion, Danagher, & Ron, 1996).

Heparanase is an endo-β-D-glucuronidase which can cleave the HS chains from HSPGs (Toyoshima & Nakajima, 1999). The cleavage leads to structural break-down of the BM and ECM, and facilitates tumor cell migration from tumor to blood vessels and lymphatics. The cleavage also can release HS-binding growth factors and induce important physiological processes such as angiogenesis (Fux, Ilan, Sanderson, & Vlodavsky, 2009; Nakajima, Irimura, & Nicolson, 1988; Parish, Freeman, & Hulett, 2001; Vlodavsky & Friedmann, 2001). Research has suggested that the metastatic abilities of tumor cells closely correlated with heparanase activity (Freeman & Parish, 1997; Ilan, Elkin, & Vlodavsky, 2006). Compared to nonmetastatic cells, highly metastatic tumor cells produce more heparanase. Therefore, heparanase is considered to be an important target for the treatment of tumor metastasis.

Recently, using heparin or heparin mimetics to inhibit heparanase has become a new strategy to prevent tumor invasion and metastasis. Among the reported heparanase inhibitors, sulfated polysaccharides are hotspots (Karoli et al., 2005; Parish, Freeman, Brown, Francis, & Cowden, 1999; Zhao et al., 2006). For example, phosphomannopentose sulfate (PI-88) and sulfated maltohexaose can significantly inhibit tumor growth, metastasis, and angiogenesis. Furthermore, PI-88 has been put through into clinical trials (Khasraw et al., 2010). According to these studies, it is possible that sulfated saccharides can be effective heparanase inhibitors to prevent tumor invasion and metastasis.

Here, we used β-(1→3)-D-glucan and carboxymethyl glucan as raw material to synthesize a series of derivatives. With the help of computer aided drug design (CADD), we predicted the activity of four derivatives against heparanase and tested their inhibitory activity of heparanase using a rapid colorimetric assay. One structurally novel sulfate derivative named PSC stood out as a potential heparanase inhibitor. We investigated the properties of PSC and tried to elucidate its molecular mechanism.

* Corresponding author at: Department of Life Science and Technology, China Pharmaceutical University, Tongjia-xiang 24#, 210009, Jiangsu, China.
Tel.: +86 025 83271108; fax: +86 025 83271249.
E-mail addresses: wangting_lisia@hotmail.com, yinhongping63@hotmail.com (M. Wang).
[1] Both the authors contributed equally to this work.

0144-8617/$ – see front matter © 2011 Elsevier Ltd. All rights reserved.
doi:10.1016/j.carbpol.2011.09.083

2. Materials and methods

2.1. Materials

β-(1→3)-D-Glucan and carboxymethyl glucan were bought from Yixing Desheng Pharmaceutical Co. Ltd., China. DEAE-cellulose and Sephadex G-25 were purchased from Sigma. Dextran standards (Mw 133800, 84400, 10000, 4600, and 180) were purchased from National Institute. Recombinant Human FGF-basic was bought from PeproTech. Antibodies of anti-FGFR, anti-ERK1/2, anti-JNK, anti-Akt, anti-phosphorylated FGFR, anti-phosphorylated ERK1/2, anti-phosphorylated JNK, and anti-phosphorylated Akt were purchased from Cell Signaling Technology, Inc. RIPA lysis buffer (strong) was bought from Beyotime Institute of Biotechnology. PVDF membrane was purchased from Whatman. HRP anti-rabbit IgG was purchased from Genescript. Chemiluminescence was purchased from Pierce. All other chemical reagents used were analytical grade.

2.2. Cell lines

Human umbilical vein endothelial cells (HUVECs) were obtained from ScienCell Research Laboratories and were cultured in CM medium supplemented with 5% fetal bovine serum (FBS), 1% ECGS, and antibiotics. MDA-MB-435 cells were obtained from the Shanghai Institute of Biochemistry and Cell Biology and propagated by standard tissue culture procedures in the DMEM medium supplemented with 10% FBS.

2.3. Preparation of glucan derivatives

β-(1→3)-D-Glucan was added to 1 M sulfuric acid and stirred at 90 °C for 6 h. The reaction was terminated with 1 M NaOH. After centrifugation, the supernatant was dialyzed with distilled water and concentrated under reduced pressure. The sample was then loaded to a column of Sephadex G25 (1.0 cm × 80 cm) and eluted with distilled water at a flow rate of 0.2 mL/min. One fraction of approximately 8,000 Da was pooled and freeze-dried. PSC was obtained by reacting with $ClSO_3H$ in pyridine at 100 °C for 3 h with stirring. PSC1 was obtained by reacting with $ClSO_3H$ in pyridine at 60 °C for 3 h with stirring. The reaction was terminated with 4 M NaOH and adjusted to pH 7.0. After desalination with dialysis and concentration under reduced pressure, the sample was loaded to a column of DEAE-cellulose 52 (2.5 cm × 30 cm). The NaCl aqueous solution (0–2 M) was eluted gradually and monitored by UV absorption at 250 nm. The product fraction was pooled, desalted, and freeze-dried.

2.4. Preparation of carboxymethyl glucan derivatives

Carboxymethyl glucan was added to 1 M sulfuric acid and stirred at 90 °C for 6 h. The reaction was terminated with 1 M NaOH. After centrifugation, the supernatant was dialyzed with distilled water and concentrated under reduced pressure. The sample was then loaded to a column of Sephadex G25 (1.0 cm × 80 cm) and eluted with distilled water at a flow rate of 0.2 mL/min. One fraction of approximately 8,000 Da was pooled and freeze-dried. PMC was obtained by reacting with $ClSO_3H$ in pyridine at 100 °C for 6 h with stirring. PMC1 was obtained by reacting with $ClSO_3H$ in pyridine at 60 °C for 6 h with stirring. The reaction was terminated with 4 M NaOH and adjusted to pH 7.0. After desalination with dialysis and concentration under reduced pressure, the sample was loaded to a column of DEAE-cellulose 52 (2.5 cm × 30 cm). The NaCl aqueous solution (0–2 M) was eluted gradually and monitored by UV absorption at 250 nm. The product fraction was pooled, desalted, and freeze-dried.

2.5. Structure characterization

Elemental analysis was detected on Elementa Vario EL III analyzer. The molecular weight was determined by a gel chromatographic technique (Rodriguez & Vanderwieles, 1979). The homogeneity was confirmed on the Agilent 1100 HPLC system equipped with a Waters Ultrahydrogel™ 2000 and an Ultrahydrogel™ 250 column (7.8 mm × 300 mm) according to the gel permeation chromatography protocol as previously described (Yang et al., 2005). The GPC software was used to generate a raw standard curve and then calculate molecular weight. The HPLC system was pre-calibrated with Dextran standards (Mw 133800, 84400, 10000, 4600, and 180).

The samples were prepared by the KBr-disk method. The IR spectrum was recorded using air as the reference. The ^{13}C spectrum was carried out with D_2O at 300 K in a Bruker AV-500 instrument using acetone as internal standard (*d* 31.01 ppm).

2.6. Computational docking

According to Maria and Jeffry's studies, we chose the xylanase from *Penicillium simplicissimum* (Protein Data Bank entry number 1BG4) as a template and downloaded from the Protein Data Bank (http://www.rcsb.org) (Zhou, Bates, & Madura, 2006). The amino acid residues from Phe 100 to Phe 410 of human heparanase sequence were used. The homology protein search was carried out using the PSI-BLAST and PHI-BLAST server at NCBI (http://www.ncbi.nlm.nih.gov/BLAST/). The SYBYL program version 7.3 and Suflex–Dock was used to dock the compounds to the active site of the enzyme (Ishida et al., 2004).

2.7. Heparanase activity assay

Human heparanase was extracted and purified as previously reported and its activity toward fondaparinux was determined as previously described (Freeman & Parish, 1998; Hammond, Li, & Ferro, 2010). The assay solution composed of 40 mM sodium acetate buffer (pH 5.0), 100 μM fondaparinux, and 140 pm heparanase with or without test sample was added to 96-well plates. After incubating at 37 °C for 24 h the reactions were stopped by 100 μL of 1.69 mM WST-1 in 0.1 M NaOH. The plates were resealed with adhesive tape and developed at 60 °C for 60 min, and the absorbance was measured at 584 nm. The IC_{50} was determined using the method of Cheng and Prusoff with GraphPad Prism 5 software (Cheng & Prusoff, 1973).

2.8. MDA-MB-435 migration assay

The effect of PSC on bFGF-induced MDA-MB-435 migration was assayed using a modified Boyden chamber technique (Cao et al., 1998). Transwell chamber membranes (8 μm thick, 8-μm pores) were used. 1% FBS and 60 ng/mL bFGF were added to the lower chambers. 1×10^5 cells per well with various concentrations of PSC were added to the upper chamber and incubated at 37 °C for 10 h in a CO_2 incubator. Cells that had not migrated were removed from the upper chamber with a cotton swab. Those attached to the filter were fixed with methanol and stained with 0.1% crystal violet. Photographs were taken under a microscope and the cells that had migrated through the filter were counted under a light microscope and plotted as numbers of migrating cells per optic field.

2.9. HUVECs migration assay

The effect of PSC on bFGF-induced HUVECs migration was also assayed using a modified Boyden chamber technique. Transwell chamber membranes (8 μm thick, 8-μm pores) were used. 1% FBS

A

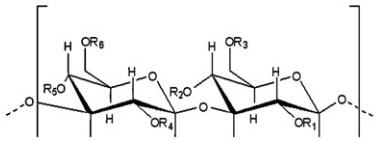

Molecular	Docking Unit						DS	Score	IC50(μg/mL)
	R_1	R_2	R_3	R_4	R_5	R_6			
PSC1	H	H	SO_3Na	H	H	SO_3Na	1.1	10.43	3.5
PSC	SO_3Na	SO_3Na	SO_3Na	SO_3Na	H	SO_3Na	2.6	6.62	0.4
PMC1	H	H	SO_3Na	H	H	CH_2COONa	0.9	2.11	>1000
PMC	SO_3Na	SO_3Na	SO_3Na	SO_3Na	H	CH_2COONa	1.9	1.98	>1000
Substarte	GlcA-GlcNAc							7.12	ND

B

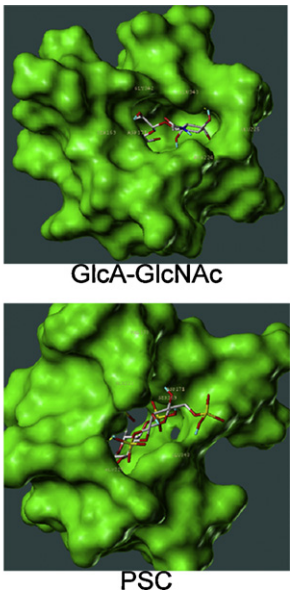

Fig. 1. Structures of β-(1→3)-D-glucan derivatives and docking results. (A) Table lists the structures, docking scores, substitution degrees and IC_{50} values of heparanase. ND, no determined. (B) Stereo view of the structures of heparanase with PSC and GlcA–GlcNAc.

and 60 ng/mL bFGF were added to the lower chambers. Non-treated cells served as a negative control. 1.8×10^5 cells per well with different concentrations of PSC were seeded in each upper chamber. After incubation for 6 h at 37 °C, cells attached to the filter were fixed in methanol and stained with 0.1% crystal violet. The cells that had migrated through the filter were counted under a light microscope and plotted as numbers of migrating cells per optic field.

2.10. Western blot analysis

HUVECs were seeded at 7×10^5 cells per well in 6-well plates. After 10 h, the growth medium was replaced with 200 μL serum-depleted medium overnight. The compound was diluted in ECM medium without serum and incubated at 37 °C for 1 h. After stimulation with 40 ng/mL bFGF and incubated for an additional 5 min, the cells were washed with cold PBS and lysed with 100 μL lysis buffer (RIPA lysis buffer, strong) on ice. Samples were collected and first separated by 10% SDS-PAGE and then transferred to a PVDF membrane. The membranes were blocked with 5% milk in PBS for 1 h, incubated for 14 h at 4 °C with primary antibody, either anti-FGFR, anti-ERK1/2, anti-JNK, anti-Akt, anti-phosphorylated FGFR, anti-phosphorylated ERK1/2, anti-phosphorylated JNK, or anti-phosphorylated Akt. They were then probed with secondary HRP anti-rabbit IgG for 1 h at 37 °C. After extensive washing with PBST, the target proteins were identified on the membranes by enhanced chemiluminescence.

3. Results

3.1. Preparation of derivatives

β-(1→3)-D-Glucan was degraded to fractions of approximately 8000 Da using sulfuric acid. The sample was sulfonated using modified Wolfrom's method and then fractionated by charge using a DEAE-cellulose column. Two sulfated derivatives (PSC1 and PSC) were obtained. Carboxymethyl glucan was degraded using sulfuric acid, sulfonated using modified Wolfrom's method and then fractionated by charge using a DEAE-cellulose column. The compounds obtained were named PMC1 and PMC.

3.2. Structure characterization

Homogeneity and molecular weight analysis of each derivative revealed that the total sugar content is above 99.0% in HPLC analysis and the GPC profile showed a single and symmetrically sharp peak. These results indicated that each derivative is a homogeneous polysaccharide with an average molecular weight of 8,000 Da. The degree of sulfate substitution per sugar residue (DS) calculated from the result of the Element analysis was listed in Fig. 1A.

IR and NMR spectroscopy were next performed on PSC and glucan. IR spectrum of PSC (Fig. 2A) shows the appearance of characteristic C–S–O bond-stretching absorption at 807 cm^{-1} and S=O bond-stretching absorptions at 1210 cm^{-1}. However, these two absorptions were absent in the spectrum of glucan, which proved that the PSC was glucan sulfate. The ^{13}CNMR spectrum of PSC (Fig. 2B) was very complicated. It shows the chemical shifts of C-6, C-2 and C-4. The complete shift of peak at C-6 from $\delta = 62.7$ to 69.9 indicated the relatively high substitution degree at C-6 position. The peak of C-2 partially shifts from $\delta = 73.3$ to 80.1. The peak of C-4 partially shifts from $\delta = 70.9$ to 75.9. The spectrum indicated that substitutions also have occurred at C-2 and C-4 position.

3.3. Docking studies on heparanase

Structure of the xylanase from *Penicillium simplicissimum* (Protein Data Bank entry number 1BG4) was used as a template of homology modeling. The study showed that the residues Glu225 and Glu343 can interact with a substrate and affect the heparanase catalysis of the substrate. Docking scores of PSC, PSC1, PMC and PMC1 were showed in Fig. 1A. The scores of two sulfated derivatives (PSC1 and PSC) are 10.43 and 6.62 separately. The scores of two carboxymethylated derivatives (PMC1 and PMC) are 2.11 and 1.98. The heparan sulfate dimer, GlcA–GlcNAc gave a score of 7.12. The three-dimensional structures of compound-heparanase complexes were showed in Fig. 1B.

3.4. Inhibitory activity of PSC and suramin against heparanase

We used a colorimetric assay for heparanase activity based on the cleavage of the synthetic heparin oligosaccharide-fondaparinux. Reducing disaccharides produced by the cleavage

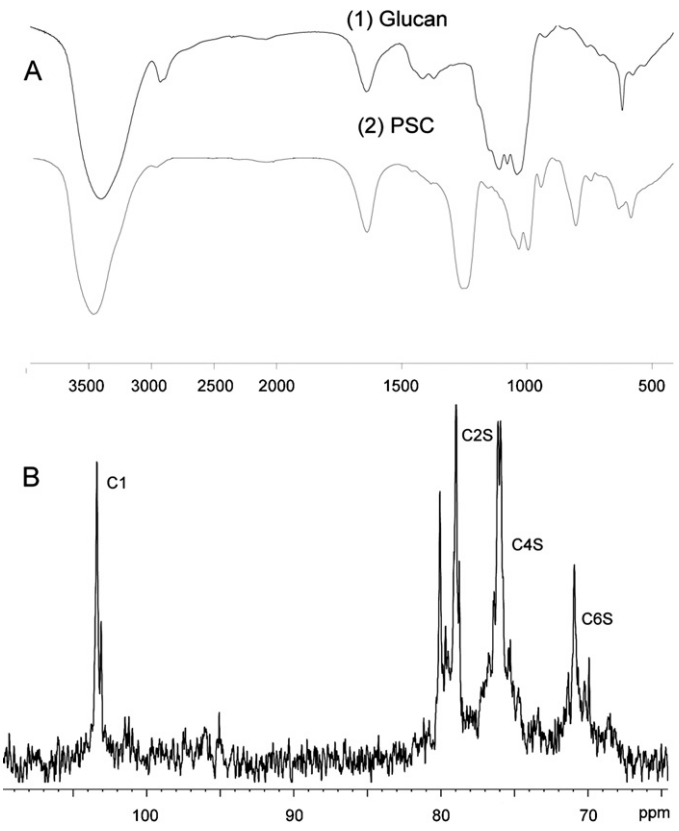

Fig. 2. Characterization of PSC. (A) IR spectra of PSC and glucan. (B) ^{13}C NMR spectrum of PSC.

can react with tetrazolium salt (WST-1) and give an absorbance at 584 nm. The IC_{50} values of four compounds were listed in Fig. 1. Fig. 3 shows that PSC inhibited heparanase enzymatic activity in a dose-dependent manner. 1.6 μg/mL PSC yielded a maximal inhibitory efficacy of 95.9%. The IC_{50} of the positive control, suramin, was 3.2 μg/mL.

3.5. Effect of PSC against bFGF induced migration

PSC inhibited the bFGF induced migration of MDA-MB-435 in a dose-dependent manner. The IC_{50} value was 0.98 μg/mL (Fig. 4). PSC remarkably inhibited the bFGF induced migration of HUVECs in a dose-dependent manner. 8 μg/mL PSC yielded an inhibitory efficacy of 84.37% (Fig. 5A). The IC_{50} value of PSC was 18.3 ng/mL.

3.6. PSC inhibit the phosphorylation of ERK1/2 and JNK

As showed in Fig. 5B, stimulation of HUVEC with bFGF (60 ng/mL) activated the phosphorylation of FGFR, ERK1/2 and JNK when compared with the blank, but it did not activate phosphorylation of Akt. Treatment with PSC had no influence on the phosphorylation of FGFR. However, PSC decreased the phosphorylation of ERK1/2 and JNK in a dose-dependent manner, which was consistent with effects of PSC on bFGF-induced HUVEC migration.

4. Discussion

Cancer chemotherapy has been one of the major medical advances in the last few decades. Most of the anticancer drugs can only kill cancer cells and shrink tumors, which have little to do with tumor metastasis and invasion processes. However, a great number of late-stage patients died of metastasis and invasion, not the primary tumor. The invasion and metastasis of tumors involve certain enzymes such as matrix metalloproteinase and heparanase in the process of destroying and remodeling ECM and BM (Huang et al., 2009). The metastatic potential of tumor cells is also correlated to the expression level of these enzymes. Some studies pointed out that the heparanase inhibitors markedly reduced the incidence of metastasis both *in vitro* and *in vivo*. Heparanase can also release some angiogenic factors such as bFGF and VEGF, both of which are bound to heparin sulfate and stored in the microenvironment around tumors. Thus, heparanase is considered to be a critical component of the angiogenic switch promoting tumor vascularization and growth. This implies that the inhibitors of heparanase may be important candidates for cancer therapy.

In a previous study, it was found that some glucan derivatives exhibited diverse biological activities such as antiviral and antitumor properties (Chihara, Hamuro, Maeda, Arai, & Fukuoka, 1970; Wang, Zhang, Li, Hou, & Zeng, 2004). Sulfation and carboxylmethylation are common in the modification of polysaccharides to enhance solubility and activity. Therefore we chose β-(1→3)-D-glucan as a backbone molecule and synthesized a series of sulfated derivatives and carboxylmethylated derivatives. We used the X-ray structure of the xylanase as the template and constructed a three-dimensional structure of heparanase from homology modeling. We docked the disaccharide units of each derivative to the TIM-barrel binding pocket of the modeled heparanase using the SYBYL program version 7.3. PMC1 and PMC gained much lower scores than GlcA–GlcNAc because of the collision between the carboxymethyl group and binding pocket. This indicated that the carboxymethylated derivatives might have no inhibitory activity against heparanase. Two sulfated derivatives (PSC1 and PSC) had scores of 10.43 and 6.62, which are equal to or better than the score of GlcA–GlcNAc. We presumed these molecules had potential inhibitory activity.

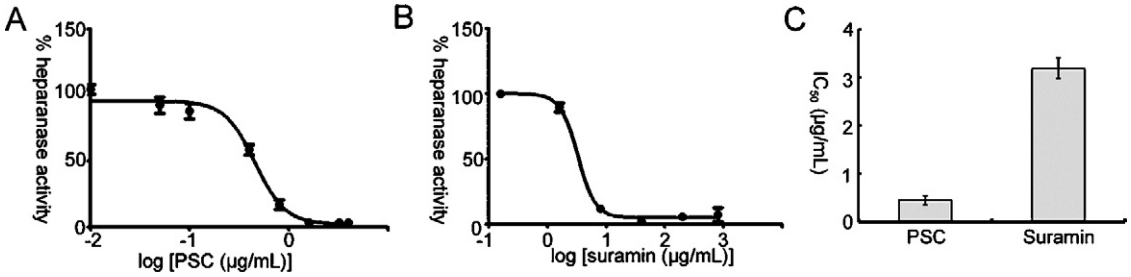

Fig. 3. Effect of PSC and suramin on heparanase. (A) PSC competitively inhibited the activity of heparanase. The curve gives an IC_{50} of 0.45 μg/mL. Data are expressed as percentages relative to controls containing no PSC. (B) The inhibition of heparanase by Suramin. The curve gives an IC_{50} of 3.2 μg/mL. Error bars are standard errors ($n = 2$). (C) The comparison of PSC and suramin.

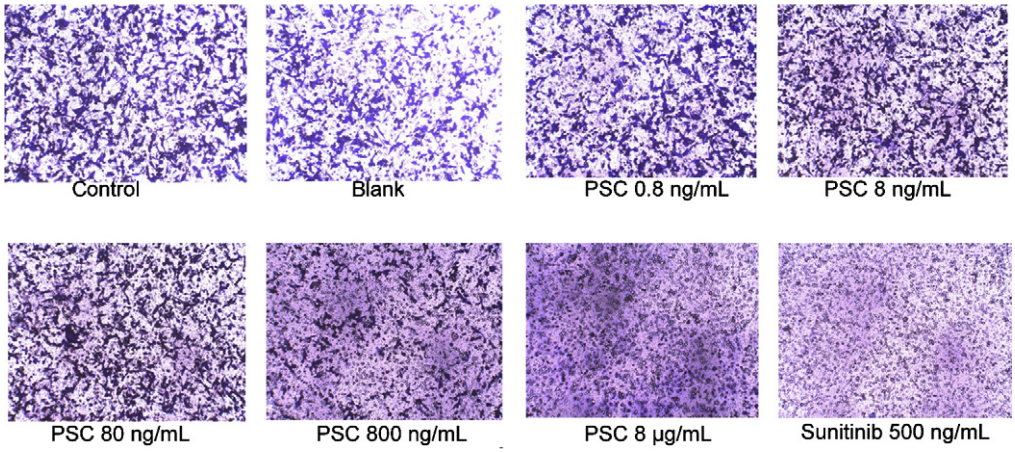

Fig. 4. Effect of PSC on bFGF induced migration of MDA-MB-435. The stimulated cells were treated with different concentrations of PSC. The concentrations are 0.8 ng/mL, 8 ng/mL, 80 ng/mL, 800 ng/mL and 8 μg/mL. Control groups were stimulated with 60 ng/mL bFGF and without PSC. Positive control group were stimulated with 500 ng/mL sunitinib. Blank group were treated without bFGF and PSC. The IC_{50} value is 0.98 μg/mL.

The heparanase activity assay *in vitro* showed that PMC1 and PMC did not have inhibitory activity against heparanase. PSC inhibited heparanase activity with an IC_{50} value of 0.4 μg/mL and PSC1 inhibited heparanase activity with an IC_{50} value of 3.2 μg/mL. These data are generally consistent with the calculation result of docking. A further study on the homology model of heparanase will be needed to improve the accuracy of docking calculation. Considering the higher inhibitory activity of PSC, we chose PSC as a candidate for further studies.

We singled out PSC and carried out a series of studies of activities and molecular mechanism of PSC. PSC has a molecular weight of about 8,000 Da. It is described as a β-(1→3)-D-glucan with an average of 2.6 sulfates substitution per sugar residue (Fig. 1A). The structural similarities between PSC and heparan sulfate, a natural substrate of heparanase, indicates PSC might be a potential

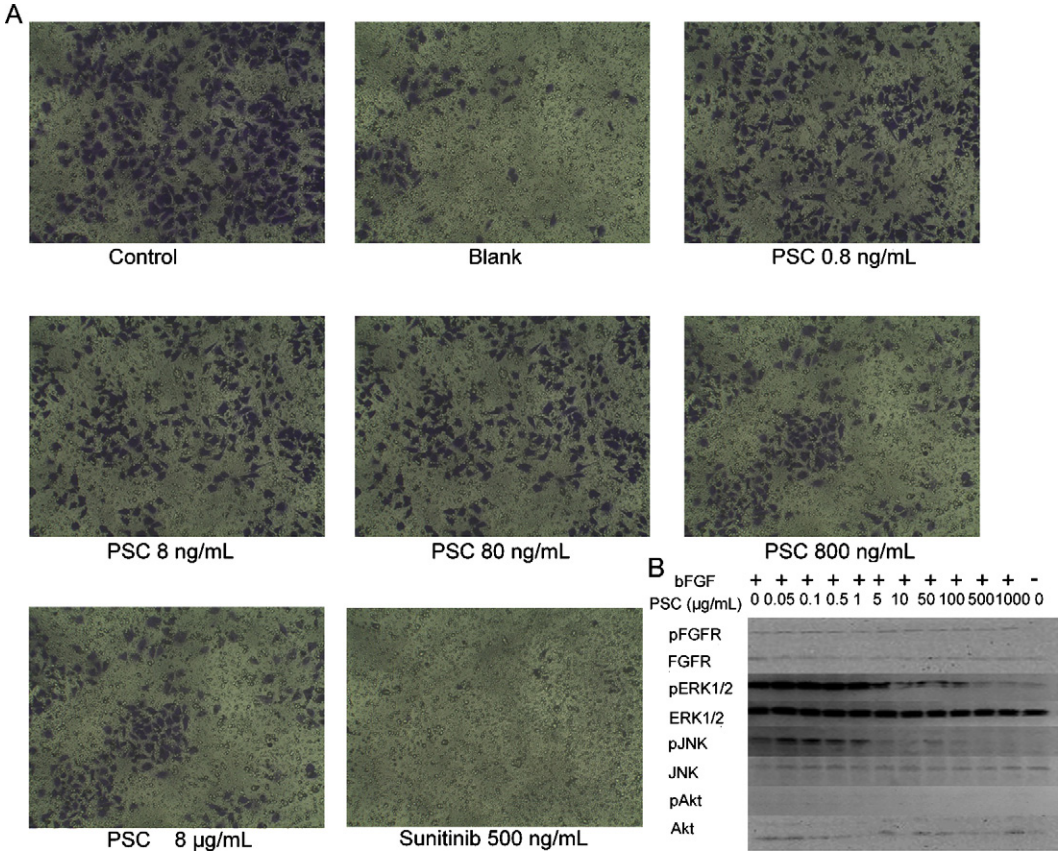

Fig. 5. Effect of PSC on bFGF-induced HUVECs migration. (A) The stimulated cells were treated with different concentrations of PSC. The concentrations are 0.8 ng/mL, 8 ng/mL, 80 ng/mL, 800 ng/mL and 8 μg/mL. Controls group were stimulated with 60 ng/mL bFGF and without PSC. Positive control group were stimulated with 500 ng/mL sunitinib. Blank group were treated without bFGF and PSC. The stimulated cells were treated with different concentrations of PSC. The IC_{50} value is 18.3 ng/mL. (B) Western blotting analysis of PSC on the phosphorylation of bFGF receptor (FGFR), ERK1/2, JNK and Akt. The concentrations of PSC are from left to right, 0, 0.05, 0.1, 0.5, 1, 5, 10, 50, 100, 500 and 1000 μg/mL. HUVECs were treated with bFGF (+) and without bFGF (−).

competitive inhibitor of heparanase. Consistent with the docking results, a further study on the heparanase activity assay showed that PSC inhibited heparanase enzymatic activity in a dose-dependent manner. The IC_{50} value of PSC was 0.4 μg/mL, while the IC_{50} of the positive control-suramin was 3.5 μg/mL. PSC showed about ten-fold higher inhibitory activity than suramin *in vitro*.

In further investigations, we found that PSC can remarkably inhibit the bFGF induced migration of HUVEC with an IC_{50} value of 18.3 ng/mL. In addition, PSC also inhibited the bFGF induced migration of MDA-MB-435 (IC_{50} = 0.98 μg/mL). It was reported that HS or heparin is very important for full FGF signaling. A ternary complex of FGF–FGFR–heparin is required to activate a series of downstream cytoplasmic signaling cascades which are important to angiogenesis (Harmer, 2006). The mitogen-activated protein-kinase (MAPK) and phosphoinositide 3-kinases (PI3K) signaling pathway are involved in bFGF-mediated endothelial cell proliferation and migration angiogenesis (Huang et al., 2009; Tanaka, Abe, & Sato, 1999). In our study, HUVECs stimulated with bFGF (60 ng/mL) might only activate ERK-1/2 and JNK while Akt remained inactivated. PSC decreased the phosphorylation of ERK 1/2 and JNK in a dose-dependent manner. Combined with the inhibitory effects of PSC on the migration of HUVECs *in vitro*, this suggests that PSC might inhibit the bFGF signal transduction pathway through the MAP kinase pathway via ERK and JNK.

5. Conclusions

In this work, four derivatives with different substitution were prepared from β-(1→3)-D-glucan or carboxymethyl glucan using modified Wolfrom's method. The structures were characterized by FTIR and ^{13}C NMR. FTIR spectra showed the characteristic absorptions of sulfate ester bonds at 807 cm^{-1} and 1210 cm^{-1}. ^{13}C NMR spectrum indicated the relatively high substitution degree at C-6 position. The docking results of four candidates predicted that PSC and PSC1 might have a potential inhibitory activity against heparanase. The result of heparanase assay *in vitro* supported the computer prediction. Of these, PSC, a sulfated glucan (8,000 Da) showed the high inhibitory activity. In further investigations, it was found that PSC remarkably inhibited the bFGF induced migration of HUVECs and MDA-MB-435. The result of the Western blotting revealed that PSC blocked basic fibroblast growth factor (bFGF) signal transduction pathway by decreasing the phosphorylation of ERK 1/2 and JNK. Further study will be needed to evaluate the activity of PSC *in vivo* and measure the interaction between PSC and bFGF and/or heparanase with the aim of developing PSC into an anti-metastatic drug candidate.

Acknowledgment

This work was supported by Jiangsu Simcere Pharmaceutical R&D Co. Ltd.

References

Cao, Y., Linden, P., Farnebo, J., Cao, R., Eriksson, A., Kumar, V., Qi, J. H., Claoesson-Welsh, H. & Alitalo, K. (1998). Vascular endothelial growth factor C induces angiogenesis in vivo. *PNAS*, *95*, 14389–14394.

Cheng, Y. & Prusoff, W. H. (1973). Relationship between the inhibition constant (K1) and the concentration of inhibitor which causes 50 per cent inhibition (IC50) of an enzymatic reaction. *Biochemical Pharmacology*, *22*, 3099–3108.

Chihara, G., Hamuro, J., Maeda, Y., Arai, Y. & Fukuoka, F. (1970). Antitumor polysaccharide derived chemically from natural glucan (pachyman). *Nature*, *225*, 943–944.

Freeman, C. & Parish, C. R. (1997). A rapid quantitative assay for the detection of mammalian heparanase activity. *Biochemical Journal*, *325*, 229–237.

Freeman, C. & Parish, C. R. (1998). Human platelet heparanase: Purification, characterization and catalytic activity. *Biochemical Journal*, *330*, 1341–1350.

Fux, L., Ilan, N., Sanderson, R. D. & Vlodavsky, I. (2009). Heparanase: Busy at the cell surface. *Trends in Biochemical Sciences*, *34*, 511–519.

Hammond, E., Li, C. P. & Ferro, V. (2010). Development of a colorimetric assay for heparanase activity suitable for kinetic analysis and inhibitor screening. *Analytical Biochemistry*, *396*, 112–116.

Harmer, N. J. (2006). Insights into the role of heparan sulphate in fibroblast growth factor signaling. *Biochemical Society Transactions*, *34*, 442–445.

Huang, S. C., Sheu, B. C., Chang, W. C., Cheng, C. Y., Wang, P. H. & Lin, S. (2009). Extracellular matrix proteases—Cytokine regulation role in cancer and pregnancy. *Frontiers in Bioscience*, *14*, 1571–1588.

Ilan, N., Elkin, M. & Vlodavsky, I. (2006). Regulation, function and clinical significance of heparanase in cancer metastasis and angiogenesis. *International Journal of Biochemistry and Cell Biology*, *38*, 2018–2039.

Ishida, K., Hirai, G., Murakami, K., Teruya, T., Simizu, S., Sodeoka, M., et al. (2004). Structure-based design of a selective heparanase inhibitor as an antimetastatic agent. *Molecular Cancer Therapy*, *3*, 1069–1077.

Jackson, R. L., Busch, S. J. & Cardin, A. D. (1991). Glycosaminoglycans: Molecular properties, protein interactions and role in physiological processes. *Physiological Reviews*, *71*, 481–539.

Karoli, T., Liu, L., Fairweather, J. K., Hammond, E., Li, C. P., Cochran, S., et al. (2005). Synthesis, biological activity, and preliminary pharmacokinetic evaluation of analogues of a phosphosulfomannan angiogenesis inhibitor (PI-88). *Journal of Medicinal Chemistry*, *48*, 8229–8236.

Khasraw, M., Pavlakis, N., McCowatt, S., Underhill, C., Begbie, S., de Souza, P., et al. (2010). Multicentre phase I/II study of PI-88, a heparanase inhibitor in combination with docetaxel in patients with metastatic castrate-resistant prostate cancer. *Annals of Oncology*, *21*, 1302–1307.

Kjellen, L. & Lindahl, U. (1991). Proteoglycans: Structures and interactions. *Annual Review of Biochemistry*, *60*, 443–475.

Nakajima, M., Irimura, T. & Nicolson, G. L. (1988). Heparanases and tumor metastasis. *Journal of Cellular Biochemistry*, *36*, 157–167.

Parish, C. R., Freeman, C., Brown, K. J., Francis, D. J. & Cowden, W. B. (1999). Identification of sulfated oligosaccharide-based inhibitors of tumor growth and metastasis using novel in vitro assays for angiogenesis and heparanase activity. *Cancer Research*, *59*, 3433–3441.

Parish, C. R., Freeman, C. & Hulett, M. D. (2001). Heparanase: A key enzyme involved in cell invasion. *Biochimica et Biophysica Acta*, *1471*, M99–M108.

Rodriguez, H. J. & Vanderwieles, A. J. (1979). Molecular weight determination of commercial heparin sodium USP and its sterile solutions. *Journal of Pharmaceutical Sciences*, *68*, 588–591.

Tanaka, K., Abe, M. & Sato, Y. (1999). Roles of extracellular signal-regulated kinase 1/2 and p38 mitogen-activated protein kinase in the signal transduction of basic fibroblast growth factor in endothelial cells during angiogenesis. *Japanese Journal of Cancer Research*, *90*, 647–654.

Toyoshima, M. & Nakajima, M. (1999). Human heparanase: Purification, characterization, cloning, and expression. *Journal of Biological Chemistry*, *274*, 24153–24160.

Vlodavsky, I. & Friedmann, Y. (2001). Molecular properties and involvement of heparanase in cancer metastasis and angiogenesis. *Journal of Clinical Investigation*, *108*, 341–347.

Vlodavsky, I., Miao, H. Q., Medalion, B., Danagher, P. & Ron, D. (1996). Involvement of heparan sulfate and related molecules in sequestration and growth promoting activity of fibroblast growth factor. *Cancer and Metastasis Reviews*, *15*, 177–186.

Wang, Y., Zhang, L., Li, Y., Hou, X. & Zeng, F. (2004). Correlation of structure to antitumor activities of five derivatives of a beta-glucan from Poria cocos sclerotium. *Carbohydrate Research*, *339*, 2567–2574.

Yang, X. B., Gao, X. D., Han, F., Xu, B. S., Song, Y. C. & Tan, R. X. (2005). Purification, characterization and enzymatic degradation of YCP, a polysaccharide from marine filamentous fungus Phoma herbarum YS4108. *Biochimie*, *87*, 747–754.

Yurchenco, P. D. & Schittny, J. C. (1990). Molecular architecture of basement membrane. *FASEB Journal*, *4*, 1577–1590.

Zhao, H., Liu, H., Chen, Y., Xin, X., Li, J., Hou, Y., et al. (2006). Oligomannurarate sulfate, a novel heparanase inhibitor simultaneously targeting basic fibroblast growth factor, combats tumor angiogenesis and metastasis. *Cancer Research*, *66*, 8779–8787.

Zhou, Z., Bates, M. & Madura, J. D. (2006). Structure modeling, ligand binding, and binding affinity calculation (LR-MM-PBSA) of human heparanase for inhibition and drug design. *Proteins*, *65*, 580–592.